J. Chem. Sci., Vol. 122, No. 3, May 2010, pp. 321–333.

Anaerobic DNA cleavage in red light by dicopper(II) complexes on disulphide bond activation

DEBOJYOTI LAHIRI[a], RITANKAR MAJUMDAR[b], ASHIS K PATRA[a] and AKHIL R CHAKRAVARTY[a,*]

[a]Department of Inorganic and Physical Chemistry, Indian Institute of Science, Bangalore 560 012
[b]Department of Molecular Reproduction, Development and Genetics, Indian Institute of Science, Bangalore 560 012
e-mail: arc@ipc.iisc.ernet.in

MS received 11 May 2009; accepted 7 July 2009

Abstract. Binuclear complexes $[Cu(\mu\text{-RSSR})]_2$ (**1**) and $[M_2(\mu\text{-PDS})(H_2O)]_2$ (M = Cu(II), **2**; Fe(II), **3**), where H_2RSSR is a reduced Schiff base derived from 2-(thioethyl)salicylaldimine having a disulphide moiety and H_2PDS is derived from dimerization of D-penicillamine, have been prepared, structurally characterized, and their photo-induced DNA cleavage activity studied. The crystal structure of **1** shows the complex as a discrete binuclear species with each metal in a CuN_2O_2 square-planar geometry (Cu…Cu, 6·420 Å). The tetradentate $RSSR^{2-}$ acts as a bridging ligand. The sulphur atoms in the disulphide unit do not interact with the metal ions. Complexes **1–3** do not show any DNA cleavage activity in darkness. The copper(II) complexes exhibit chemical nuclease activity in the presence of 3-mercaptopropionic acid. Cleavage of supercoiled DNA has been observed in UV-A light of 365 nm for **1** and red light of 647·1 nm for both **1** and **2** in air. Mechanistic data reveal the involvement of the disulphide unit as photosensitizer generating hydroxyl radicals ($^{\bullet}$OH) as the reactive species. Photo-induced DNA cleavage in red light seems to involve sulphide radicals in a type-I process and hydroxyl radicals. The dicopper(II) complexes show significant anaerobic photo-induced DNA cleavage activity in red light under argon following type-I pathway without involving any reactive oxygen species.

Keywords. Dicopper(II) complexes; anaerobic DNA photo-cleavage; crystal structure; disulphide bond activation; D-penicillamine disulphide.

1. Introduction

The antibiotics derived from natural products containing thio-moieties and their synthetic analogues have been used in DNA cleavage studies.[1–9] The nuclease activity of compounds having thio moieties generally follows thiol-dependent cleavage pathway in which a Fenton-type reaction activates molecular oxygen to form hydroxyl radical as the DNA cleaving agent. The antitumor, antibiotic leinamycin and its analogues are known as 'chemical nucleases' forming reactive hydroxyl species.[8,9] Earlier reports from our laboratory have shown that redox active copper(II) complexes having ligands with thioalkyl moieties are efficient DNA-cleaving agents on treatment with either a reducing agent or on photoactivation.[10,11] Photo-induced DNA cleavage by ternary copper(II) complexes having a metal-bound thioalkyl moiety is known to be metal-assisted involving sulphur-to-copper charge transfer band and the metal-based *d–d* band forming singlet oxygen in a type-II pathway.[11] Compounds showing red-light-induced DNA cleavage activity are of importance considering their potential use in the chemistry of photodynamic therapy (PDT) of cancer.[12–14] The currently used PDT drug is Photofrin® which is a porphyrin-based compound that causes DNA damage at 630 nm.[15–17] Organic dyes like porphyrin and phthalocyanine bases are known to show oxidative photo-cleavage of DNA by singlet oxygen pathway. Such compounds are active only in the presence of oxygen and become ineffective under hypoxic conditions of cancer cells. Therefore, it is of interest to design potent PDT agents that are active under hypoxic reaction conditions.

The present work stems from our continued interest to develop the chemistry of copper(II) complexes showing visible light-induced DNA cleavage acti-

*For correspondence

vity under both aerobic and anaerobic reaction conditions.[10,11,18–26] We have earlier shown that a dicopper(II) complex having a Schiff base ligand bearing a disulphide moiety is capable of cleaving DNA on photo-irradiation under argon atmosphere.[26] We have now extended the study using a reduced Schiff base ligand having a disulphide moiety and a biologically important amino acid, viz. D-penicillamine disulphide as new photosensitizers. Compounds having a disulphide bond are found to be suitable for photoactivation in visible light in a similar way as rhodopsins undergo photoactivation of the S–S bond for its biological function.[27] Besides, formation and cleavage of disulphide bonds are known to be important for the biological activity of several sulphur containing peptides and proteins.[28,29] Compounds containing disulphide linkages have also been used in mapping collagen–protein interactions.[30] Here, we report the photo-induced DNA cleavage activity of two dicopper(II) complexes, viz. $[Cu(\mu\text{-RSSR})]_2$ (**1**) and $[Cu(\mu\text{-PDS})(H_2O)]_2$ (**2**), where H_2RSSR is a reduced Schiff base derived from 2-(thioethyl)salicylaldimine having a disulphide moiety and H_2PDS is D-penicillamine disulphide, viz. 3,3′-dithiobis (2-amino-3-methylbutyric acid), obtained from dimerization of D-penicillamine (scheme 1). The significant result of this work is the anaerobic DNA cleavage activity of the complexes in red light. An analogous diiron(II) complex $[Fe(\mu\text{-PDS})(H_2O)]_2$ (**3**) is found to show poor photo-induced DNA cleavage activity under similar reaction conditions.

2. Experimental

2.1 *Materials and measurements*

All reagents and chemicals were purchased from commercial sources and used as received. Solvents used for electrochemical and spectroscopic measurements were purified by standard procedures.[31] Supercoiled (SC) pUC19 DNA (caesium chloride purified) was procured from Bangalore Genie (India). Calf thymus (CT) DNA, agarose (molecular biology grade), distamycin, catalase, methyl green, ethidium bromide (EB), 35mer single strand DNA (5′-GGGAATTCTTCCAGAGTAGGCAGCTTTTTTA AGTT) and superoxide dismutase (SOD) were from Sigma (USA). D-Penicillamine disulphide (PDS) was purchased from Aldrich (USA) and cysteamine hydrochloride from Lancaster (UK). MG 1655 total *t*-RNA was used for comparative cleavage studies. Tris(hydroxymethyl)aminomethane–HCl (Tris–HCl) buffer was prepared using deionized and sonicated triple distilled water. Complexes $[Cu(\mu\text{-PDS})(H_2O)]_2$ (**2**) and $[Fe(\mu\text{-PDS})(H_2O)]_2$ (**3**) were prepared by following a reported procedure.[32]

The elemental analysis was done using a Thermo Finnigan FLASH EA 1112 CHNS analyzer. The infrared and electronic spectra were recorded on PerkinElmer Lambda 35 and Varian Cary 300 Bio at 25°C, respectively. Magnetic susceptibility data in the temperature range 300–20 K for the polycrystalline samples of the complexes were obtained using Model 300 Lewis-coil-force magnetometer of George Associates Inc. (Berkeley, USA) make. $Hg[Co(NCS)_4]$ was used as a standard. Experimental susceptibility data were corrected for diamagnetic contributions.[33] The molar magnetic susceptibilities were fitted by Bleaney–Bowers expression by means of a least-squares program: $\chi_{Cu} = [Ng^2\beta^2/kT][3 + \exp(-2J/kT)]^{-1} + N_\alpha$.[34] Cyclic voltammetric measurements were made at 25°C on an EG&G PAR model 253 VersaStat potentiostat/galvanostat with electrochemical analysis software 270 using a three electrode set-up comprising of a glassy carbon working, platinum wire auxiliary and a saturated calomel reference electrode (SCE) in DMF–Tris–HCl buffer (2 : 1 v/v). Tetrabutylammonium perchlorate (TBAP, 0·1 M) was used as a supporting electrolyte. Electron paramagnetic resonance (EPR) spectra were obtained using Bruker EMX spectrometer. Mass spectral measurements were done in aqueous DMF on Bruker Daltonics Esquire 300 Plus Model mass spectrometer.

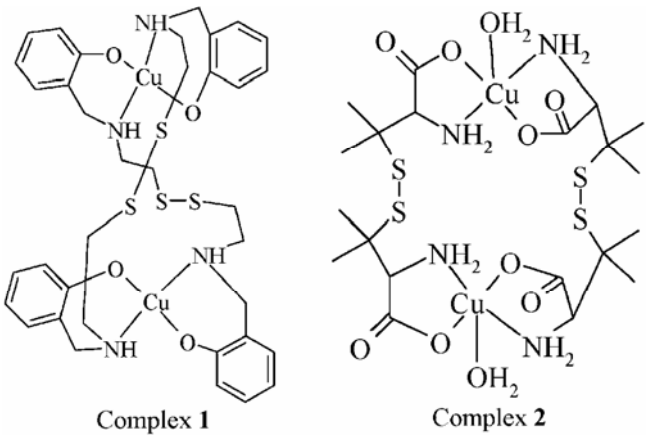

Scheme 1. Binary dicopper(II) complexes **1** and **2**.

2.2 *Preparation of the ligand bis(2-hydroxybenzylaminoethyl)disulphide (H_2RSSR)*

Ligand H_2RSSR was prepared from the reduction of the Schiff base derived from *bis*(2-(thioethyl)sali-

cylaldimine). The Schiff base (2 mmol, 0·72 g) was dissolved in 15 ml methanol. Solid sodium borohydride (4 mmol, 0·15 g) was added in portions to this solution at 0°C till the reaction mixture became ivory coloured. It was stirred for 2 h followed by removal of the solvent by rotary evaporation. The solid thus obtained was dissolved in water (20 ml) followed by an extraction of the ligand with CH_2Cl_2 (100 ml). The organic solvent was removed by rotary evaporation for isolation of the ligand. For $C_{18}H_{24}N_2O_2S_2$: ESI–MS in MeOH: *m/z* 365 $[M + H]^+$. ^1H NMR ($CDCl_3$): δ 7·2 [*t*, 2H, Ph], 7·0 [*d*, 2H, Ph], 6·8 [*m*, 4H, Ph], 4·0 [*s*, 4H, $-CH_2-N$], 3·0 [*t*, 4H, $N-CH_2-C$], 2·88 [*t*, 4H, $C-CH_2-S$].

2.3 *Preparation of [Cu(μ-RSSR)]$_2$* (**1**) *and [Cu(μ-PDS)(H$_2$O)]$_2$* (**2**)

Complex **1** was prepared by treating $Cu(NO_3)_2 \cdot 3H_2O$ (0·5 g, 2·06 mmol) taken in 5 ml of methanol with 3 ml methanol solution of tetramethylethylenediamine (0·61 ml, 4·06 mmol) that gave a dark blue colour on stirring for 30 min and subsequent addition of 9 ml dichloromethane solution of H_2RSSR (0·74 g, 2·04 mmol) to this solution was done under continuous stirring. The reaction mixture stirred for 1 h to form a green precipitate that was isolated, washed with methanol and dichloromethane, and finally with diethyl ether followed by drying over P_2O_5. The filtrate on slow evaporation gave brown rectangular block-shaped crystals (Yield: 1·23 g, 70%). For **1**, $C_{36}H_{44}Cu_2N_4O_4S_4$: C, 50·74; H, 5·20; N, 6·58; S, 15·05. Found: C, 51·09; H, 4·87; N, 6·46; S, 14·79%. ESI–MS in MeOH: *m/z* 850 $[M + H]^+$. Λ_M, S m^2 M^{-1} in DMF at 25°C: 10. FT–IR, cm^{-1} (KBr disc): 3421 *br*, 3154 *br*, 1601 *m*, 1483 *s*, 1454 *s*, 1272 *m*, 1114 *s*, 878 *w*, 761 *m*, 619 *m* (*br*, broad; *s*, strong; *m*, medium; *w*, weak). λ_{max}, nm (ε, M^{-1} cm^{-1}) in DMF: 638 (220), 418 (1750), 295 (12000). μ_{eff}, μ_B at 298 K: 1·78 (per copper(II)). Complex **2** was prepared following a reported procedure in which $CuCl_2 \cdot 2H_2O$ (1·2 mmol) was reacted with an aqueous solution (2 ml) of H_2PDS (1·2 mmol) and the excess ligand was neutralized by adding aqueous solution of $NaHCO_3$.[32] The solution was filtered and blue prismatic crystals were obtained on slow evaporation of the solvent (Yield: 75%). For **2**, $C_{20}H_{40}Cu_2N_4O_{10}S_4$: C, 31·95; H, 5·36; N, 7·45; S, 17·06. Found: C, 31·81; H, 5·58; N, 7·28; S, 16·85. ESI–MS in MeOH: *m/z* 751 $[M + H]^+$. Λ_M, S m^2 M^{-1} in DMF at 25°C: 15. FT–IR, cm^{-1} (KBr disc): 3515 *br*, 3287 *br*, 3111 *sh*, 1618 *vs*, 1377 *s*, 1110 *m*, 1050 *m*, 792 *w*, 594 *w*. λ_{max}, nm (ε, M^{-1} cm^{-1}) in DMF: 610 (70), 234 (8000). μ_{eff}, μ_B at 298 K: 1·81 (per copper(II)).

2.4 *Preparation of [Fe(μ-PDS)(H$_2$O)]$_2$* (**3**)

Complex **3** was prepared following the procedure of complex **2** from a reaction of $FeCl_2 \cdot 2H_2O$ (1·2 mmol) and H_2PDS (1·2 mmol) in methanol (5 ml) and the excess ligand was neutralized with an aqueous solution of $NaHCO_3$. The solution was filtered and the light yellow–brown precipitate was isolated, washed with methanol and diethyl ether, and finally dried *in vacuo* (Yield: 71%). For **3**, $C_{20}H_{40}Fe_2N_4O_{10}S_4$: C, 32·62; H, 5·47; N, 7·61; S, 17·42. Found: C, 32·52; H, 5·65; N, 7·34; S, 17·12. ESI–MS in MeOH: *m/z* 736 $[M + H]^+$. Λ_M, S m^2 M^{-1} in DMF at 25°C: 23. FT–IR, cm^{-1} (KBr disc): 3345 *br*, 2973 *br*, 2927 *sh*, 1621 *vs*, 1387 *s*, 1111 *s*, 1042 *s*, 774 *w*, 601 *w*. λ_{max}, nm (ε, M^{-1} cm^{-1}) in DMF: 224 (7310), 345 (2400).

2.5 *Solubility and stability*

The complexes showed good solubility in DMF, DMSO, CH_2Cl_2; moderate solubility in methanol, ethanol and less solubility in water. The complexes were soluble in aqueous DMF and Tris–HCl–DMF mixture. The complexes showed stability in the solid and solution phases.

2.6 *X-ray crystallographic procedures*

The structure of **1** was obtained by single crystal X-ray diffraction technique. Single crystals were obtained on slow evaporation of a $MeOH–CH_2Cl_2$ (1 : 2 *v/v*) solution of the complex. Crystal mounting was done on a glass fibre with epoxy cement. All geometric and intensity data were collected at room temperature using an automated Bruker SMART APEX CCD diffractometer equipped with a fine focus 1·75 kW sealed tube Mo–K_α X-ray source (λ = 0·71073 Å) with increasing ω (width of 0·3° per frame) at a scan speed of 13 s per frame. Intensity data, collected using $\omega - 2\theta$ scan mode, were corrected for Lorentz–polarization effects and for absorption.[35] Structure was solved by the combination of Patterson and Fourier techniques and refined by full-matrix least-squares method using SHELX

system of programs.[36] All hydrogen atoms belonging to the complex were in their calculated positions and refined using a riding model. All non-hydrogen atoms were refined anisotropically. Perspective view of the molecule was obtained by ORTEP.[37] Selected crystal data for the complex are summarized in table 1. Detailed crystallographic data for structural analysis have been deposited with the Cambridge Crystallographic Data Centre, CCDC reference number 705477 for **1**. Copies of this information may be obtained free of charge from The Director, CCDC, 12 Union Road, Cambridge CB2 1EZ, UK (Fax: +44-1223-336033; e-mail: deposit@ccdc.cam.ac.uk or www: http://www.ccdc.cam.ac.uk).

2.7 *DNA binding experiments*

All the experiments involving the interaction of the complexes with DNA were carried out in Tris–HCl buffer (50 mM Tris-HCl, pH 7·2) at room temperature. A solution of CT DNA in the buffer gave a ratio of UV absorbance at 260 and 280 nm of about 1·89 : 1, indicating the CT DNA sufficiently free from protein. The CT DNA concentration per nucleotide was determined by absorption spectroscopy using the molar absorption coefficient of 6600 M^{-1} cm^{-1} at 260 nm.[38] Binding experiments of the complexes to single-strand DNA were done using same experimental conditions.

Table 1. Selected crystallographic data for **1**.

Formula	$C_{36}H_{44}Cu_2N_4O_4S_4$
Fw, g M^{-1}	852·07
Crystal system	Monoclinic
Space group (no.)	*C*2/*c* (15)
a (Å)	17·422(8)
b (Å)	13·852(6)
c (Å)	18·061(8)
α °	90·00
β °	100·490(6)
γ °	90·00
V (Å^3)	4286(3)
Z	4
T (K)	293(2)
ρ_{calc} (g cm^{-3})	1·321
λ, Å (Mo-K$_\alpha$)	0·71073
μ (cm^{-1})	12·26
Data/restraints/parameters	3737/0/226
Goodness-of-fit on F^2	1·039
R (F_o)[a] (*I* > 2σ(*I*)) [*R* all data]	0·1094 [0·2340]
wR (F_o)[b] (*I* > 2σ(*I*)) [*wR* (all data])	0·1751 [0·2220]
Largest diff. peak and hole (e. Å^{-3})	0·621, –0·399
$w = 1/[\sigma^2(F_o^2)+(AP)^2+(BP)]$	A = 0·0835; B = 0·0

[a]$R = \Sigma||F_o| - |F_c||/\Sigma|F_o|$. [b]$wR = \{\Sigma[w(F_o^2 - F_c^2)^2]/\Sigma[w(F_o)^2]\}^{1/2}$, $w = [\sigma^2(F_o)^2 + (AP)^2 + BP]^{-1}$, where $P = (F_o^2 + 2F_c^2)/3$.

The absorption titration experiments were performed by varying the concentration of CT DNA or 35mer single-strand DNA (5′-GGGAATTCTT CCAGAGTAGGCAGCTTTTTTAAGTT) while keeping the dicopper(II) complex concentration as constant. Due correction was made for the absorbance of CT DNA itself. The spectra were recorded after equilibration for 5 min. The intrinsic equilibrium binding constant (K_b) and the binding site size (*s*) of the complexes to CT DNA and single strand DNA were obtained by McGhee-von Hippel (MvH) method using the expression of Bard and coworkers.[39,40] The change of the absorption intensity of the spectral band was monitored on increasing the concentration of CT DNA. The binding parameters were obtained by regression analysis of the equation: $(\varepsilon_a - \varepsilon_f)/(\varepsilon_b - \varepsilon_f) = (b - (b^2 - 2K_b^2C_t[DNA]_t/s)^{1/2})/2K_bC_t$, $b = 1 + K_bC_t + K_b[DNA]_t/2s$, where ε_a is the extinction coefficient observed for the charge transfer absorption band at a given DNA concentration, ε_f is the extinction coefficient of the complex free in solution, ε_b is the extinction coefficient of the complex when fully bound to DNA, K_b is the equilibrium binding constant, C_t is the total metal complex concentration, $[DNA]_t$ is the DNA concentration in nucleotides and *s* is the binding site size in base pairs. The nonlinear least-squares analysis was done using Origin Lab, version 6.1.

DNA melting experiments were carried out by monitoring the absorption intensity of CT DNA (160 μM) at 260 nm at various temperatures, both in the absence and presence of the dicopper(II) complexes (40 μM). Measurements were carried out using a PerkinElmer Lambda 35 spectrophotometer equipped with a Peltier temperature-controlling programmer (PTP 6) (± 0·1°C) on increasing the temperature of the solution by 0·5°C min^{-1}. Viscometric experiments were performed using Schott Gerate AVS 310 Automated Viscometer that was thermostated at 37 (± 0·1)°C in a constant temperature bath. The concentration of CT DNA was 120 μM in NP. The flow times were measured with an automated timer. Each sample was measured 3 times and an average flow time was calculated. The relative solution viscosity (η/η_0) was estimated from the relation $(L/L_0) = (\eta/\eta_0)^{1/3}$, where (L/L_0) is the contour length and L_0, η_0 denote the apparent molecular length and solution viscosity, respectively, in the absence of the metal complex.[41] Viscosity values were determined

from the observed flow time of DNA-containing solutions (t) corrected for that of the buffer alone (t_0), $\eta = (t - t_0)$.

2.8 *DNA and RNA cleavage study*

The cleavage of supercoiled pUC19 DNA (30 μM, 0·2 μg, 2686 base-pairs) was studied by agarose gel electrophoresis using dicopper(II) complexes **1** and **2** and diiron(II) complex **3**, in 50 mM Tris(hydroxymethyl)methane–HCl (Tris–HCl) buffer (pH 7·2) and 50 mM NaCl. The photo-cleavage of MG 1655 total *t*-RNA (60 ng per μL) was studied by agarose gel electrophoresis using dicopper(II) complexes **1** and **2**. For DNA and RNA photo-cleavage studies, the reactions were carried out under illuminated conditions using UV-A light of 365 nm (6 W, Bangalore Genie make) and visible laser light of 647·1 nm using Spectra Physics Water-Cooled Mixed-Gas Ion Laser Stabilite® 2018-RM (beam diameter at $1/e^2 = 1{\cdot}8$ mm ± 10% and beam divergence with full angle = 0·70 mrad ± 10%). The laser power was 100 mW, measured using Spectra Physics CW Laser Power Meter (Model 407A). A 2 mM solution of the complexes was prepared in DMF followed by dilution using 50 mM Tris–HCl buffer (pH 7·2) to make a 400 μM stock solution for 365 nm and 800 μM stock solution for 647·1 nm photocleavage experiments. A 2 μL solution of the complex was diluted to an overall volume of 20 μL on adding DNA or RNA solution (1 μL), 50 mM NaCl solution (1 μL) and Tris-buffer (16 μL). The final concentration of the complex solution was 40 μM for UV and 80 μM for red light experiments. Each sample was pre-incubated for 1·0 h at 37°C and then exposed to light. After light exposure, each sample was further incubated for 1·0 h at 37°C and analysed for the photo-cleaved products using gel electrophoresis. The mechanistic studies were done using different additives (NaN_3, 2 mM; DMSO, 4 μL; catalase, 4 units; SOD, 4 units) prior to the addition of the complex. For the D_2O experiment, this solvent was used to dilute the sample to 20 μL. The samples after incubation in a dark chamber were added to the loading buffer containing 25% bromophenol blue, 0·25% xylene cyanol, 30% glycerol (3 μL). The solution was finally loaded on 0·8% agarose gel containing 1·0 μg ml^{-1} ethidium bromide. Electrophoresis was done in a dark chamber for 2 h at 60 V in TAE (Tris-acetate EDTA) buffer. Bands were visualized by UV light and photographed. The extent of DNA or RNA cleavage was measured from the intensities of the bands using UVITEC Gel Documentation System. Due corrections were made for the low level of nicked circular (NC) form present in the original supercoiled (SC) DNA sample and for the low affinity of EB binding to SC compared to NC and linear forms of DNA.[42] The concentrations of the complexes and additives corresponded to that in the 20 μL final volume of the sample using Tris buffer. The observed error in measuring the band intensities ranged between 3 and 6%.

3. Results and discussion

3.1 *Synthesis, structure and general properties*

Dicopper(II) complex $[Cu(\mu\text{-RSSR})]_2$ (**1**), where H_2RSSR is a reduced Schiff base, viz. *bis* (2-hydroxybenzylaminoethyl)disulphide, has been prepared in high yield. Complex **2** has been prepared by a reported procedure from a reaction of copper(II) chloride with D-penicillamine disulphide (H_2PDS) in the presence of $NaHCO_3$ in water.[32] The diiron(II) complex **3** has been prepared by following a similar procedure and used for DNA photocleavage experiments as a control. The complexes are characterized from the analytical and spectral data (scheme 1). Selected physicochemical data are given in table 2. The non-electrolytic complexes are soluble in aqueous DMF. The IR spectrum of complex **1** shows characteristic bands for Cu–O, Cu–N and C–N at 619, 761 and 1114 cm^{-1}, respectively. Complex **2** displays Cu–O, Cu–N and C=O (carboxylate) IR bands at 594, 792 and 1618 cm^{-1}, respectively. Complex **3** shows Fe–O, Fe–N and C=O (carboxylate) IR bands at 601, 774 and 1621 cm^{-1}, respectively. The electronic absorption spectra of **1** and **2** in DMF exhibit low-energy, low-intensity metal-centered band near 610 nm (figure 1). An intense band observed at 418 nm for **1** could be due to phenolate-to-copper(II) charge transfer (LMCT) transition. The other bands appearing in the UV-region are assignable to the intraligand transitions.[43] The iron(II) complex **3** shows electronic spectral bands as 224 and 345 nm in DMF. The copper(II) complexes have one-electron paramagnetic copper(II) centers giving a magnetic moment value of ~1·8 μ_B per copper(II) at 25°C. The copper(II) centers are essentially magnetically non-interacting giving a $2J$ value of ~1·5 cm^{-1} from the variable

Table 2. Physicochemical data and DNA binding parameters for the dicopper(II) complexes.

Complex	**1**	**2**
d–d band: λ_{max}/nm (ε/M^{-1} cm^{-1})[a]	638 (220)	610 (70)
Λ_M[b]/S m^2 M^{-1}	10	15
μ_{eff}[c]/μ_B [2J, cm^{-1}]	1·78 [1·3]	1·81 [1·5]
K_b[d,e]/M^{-1} (s)	2·0(± 0·8) × 10^4 (0·5)	2·3 (±0·9) × 10^4 (0·2)
ΔT_m[f]/°C	0·4	0·2

[a]In DMF-Tris buffer (1 : 1 v/v) medium. [b]In DMF-Tris buffer (1 : 1 v/v) medium at 25°C. [c] μ_{eff} (per copper) for solid samples at 298 K. [d]Intrinsic DNA binding constant (K_b) from absorption spectral method. The binding site size is s. [e]The K_b value for the single strand 35 mer DNA is 2·3 × 10^2 M^{-1} and 1·8 × 10^2 M^{-1} for **1** and **2** respectively. [f]Changes in the melting temperature of CT DNA.

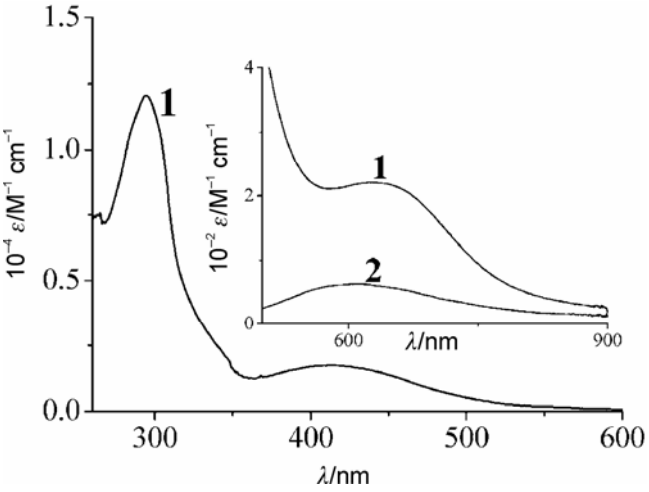

Figure 1. Electronic spectra of [Cu(μ-RSSR)]$_2$ (**1**) in DMF-Tris buffer (1 : 1 v/v) medium. The inset shows the *d–d* band of the complexes **1** and **2**.

temperature magnetic susceptibility data (figure 2). The copper(II) centers in the complexes do not show any apparent magnetic interaction as evidenced from their EPR spectra that are characteristic of non-interacting dicopper(II) complexes (figure 2). The observation of a weak half-field signal in the EPR spectrum could be due to very weak ferromagnetic interaction between the metal centers in the solid state. The rhombic nature of the spectrum suggests distortion from ideal square-planar geometry of the copper(II) centre. The complexes are redox inactive.

Complex **1** has been structurally characterized by single-crystal X-ray diffraction technique. An ORTEP view of the complex is shown in figure 3. Selected bond distances and angles are given in table 3. The structure of the complex consists of a discrete binuclear copper(II) species bonded to two dianionic N,O-donor reduced Schiff base ligands through the phenolate oxygen and secondary amine nitrogen atoms. The complex has $Cu^{II}N_2O_2$ square-planar coordination geometry. The molecule has a significantly puckered structure involving the disulphide bond. The average Cu–N distance is 2·034 Å. The average Cu–O and S–S distances are 1·910 Å and 2·047 Å respectively. The reported crystal structure of complex **2** as **2**·9H_2O has structural similarity with that of **1** except that each copper(II) center in **2** is bound to an axial aqua ligand giving CuN_2O_3 square-pyramidal coordination geometry.[32] The EPR and mass spectral data show that the dimeric structure of the complexes is retained in the solid and solution phases (figures 2 and 4).

3.2 *DNA binding properties*

We have used absorption titration method to monitor the interaction of the complexes **1** and **2** with CT DNA. Intercalation of a complex to DNA generally results in hypochromism and red shift (bathochromism) of the absorption band due to strong stacking interaction between the aromatic chromophore of the ligand and the base pairs of the DNA.[44,45] The extent of hypochromism thus gives an estimate of the strength of an intercalative binding. In absence of any DNA intercalating ligands in the present complexes, the observed red shift is small (~3 nm). The intrinsic equilibrium DNA binding constant (K_b) values of the complexes are ~2 × 10^4 M^{-1} (table 2). The small value of the binding site size (s) suggests greater surface aggregation or DNA groove binding in preference to intercalative mode of binding.[40] Binding of the complexes to single strand DNA does not show any significant shift in the absorbance

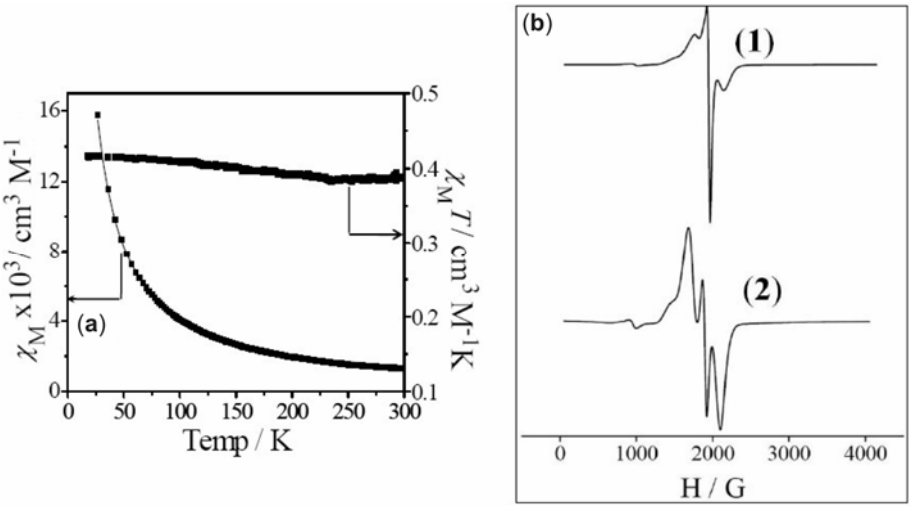

Figure 2. (**a**) Variable temperature magnetic susceptibility plot for the complex **1**. (**b**) EPR spectra of [Cu(μ-RSSR)]$_2$ (**1**) and [Cu(μ-PDS)(H_2O)]$_2$ (**2**) in the solid state.

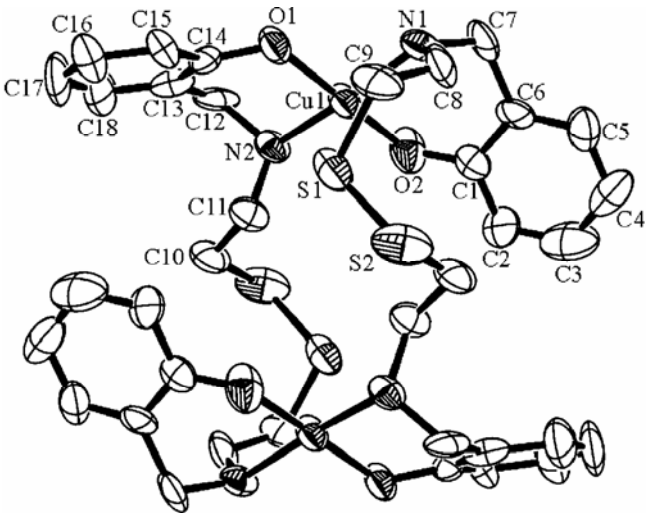

Figure 3. An ORTEP diagram of complex **1** showing 50% probability thermal ellipsoids and the atom labelling scheme.

Table 3. Selected bond distances (Å) and angles (°) for [Cu(μ-RSSR)]$_2$ (**1**).

Cu(1)–O(1)	1·916(7)	O(1)–Cu(1)–O(2)	174·0(3)
Cu(1)–O(2)	1·910(7)	O(2)–Cu(1)–N(2)	91·7(3)
Cu(1)–N(1)	2·033(7)	O(1)–Cu(1)–N(2)	84·8(3)
Cu(1)–N(2)	2·033(7)	O(2)–Cu(1)–N(1)	88·3(3)
S(1)–S(2)	2·047(5)	O(1)–Cu(1)–N(1)	94·8(3)
N(1)–C(8)	1·471(13)	N(1)–Cu(1)–N(2)	174·4(3)

maximum or any decrease in the intensity of the band. This suggests that the complexes are preferential groove or surface binder to the CT DNA and do not bind to single strand DNA.

Thermal behaviour of DNA in the presence of the complexes provides information on the conformational changes and the strength of the DNA-complex interaction. The double-stranded DNA gradually dissociates to single strands on increasing the solution temperature. The melting temperature T_m that is defined as the temperature where half of the total base pairs gets non-bonded is a valuable parameter. We have observed a small change in the DNA melting temperature (ΔT_m) on addition of the complexes to CT DNA (table 2, figure 5). The low ΔT_m value suggests primarily surface and/or groove binding propensity of the complexes to CT DNA stabilizing the DNA double helix structure.[46] Viscosity measurements are done to examine the effect on the specific relative viscosity of CT DNA upon addition of the copper(II) complexes. Since the relative specific viscosity (η/η_0) of DNA gives a measure on the increase in contour length associated with the separation of DNA base pairs due to intercalation, a DNA intercalator like ethidium bromide shows significant increase in the viscosity of the DNA solutions (η and η_0 are the specific viscosities of DNA in the presence and absence of the complexes, respectively).[47,48] The plot of relative specific viscosity $(\eta/\eta_0)^{1/3}$ versus [complex]/[DNA] ratio for the present complexes shows only minor negative change in the viscosity indicating primarily DNA surface and/or groove binding nature of the complexes (figure 6).

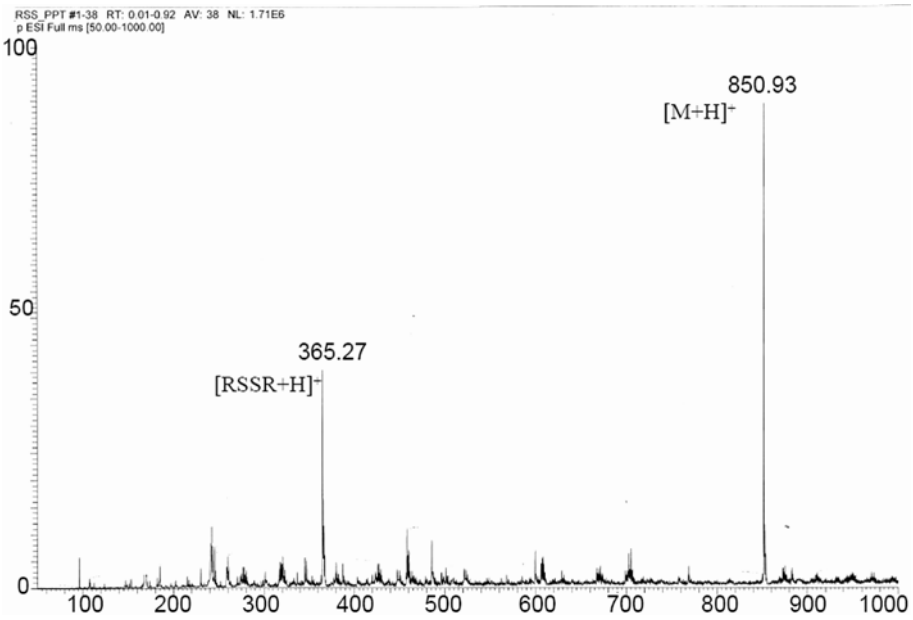

Figure 4. Mass spectrum of complex **1** in aqueous DMF (1 : 1 v/v) showing the parent ion peak at 850·93 *m/z*. The peak at 365·27 *m/z* is due to the ligand.

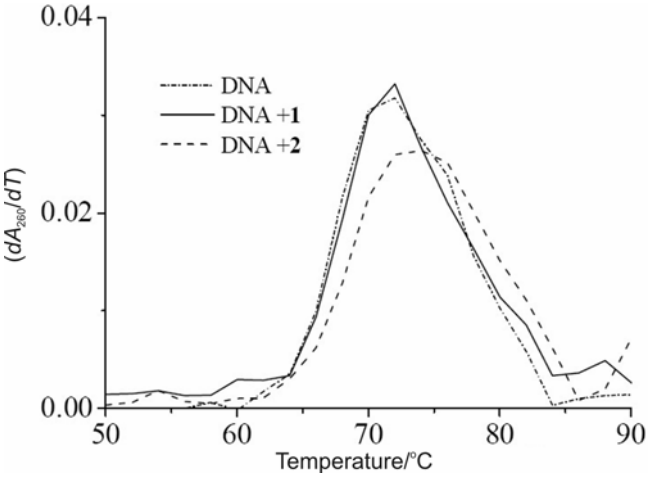

Figure 5. Effect of addition of the complexes **1** and **2** (43 μM) on the melting temperature of CT–DNA (-·-·-) (173 μM) in 5 mM phosphate buffer (pH 6·85) with a ramp rate of 0·5°C/min.

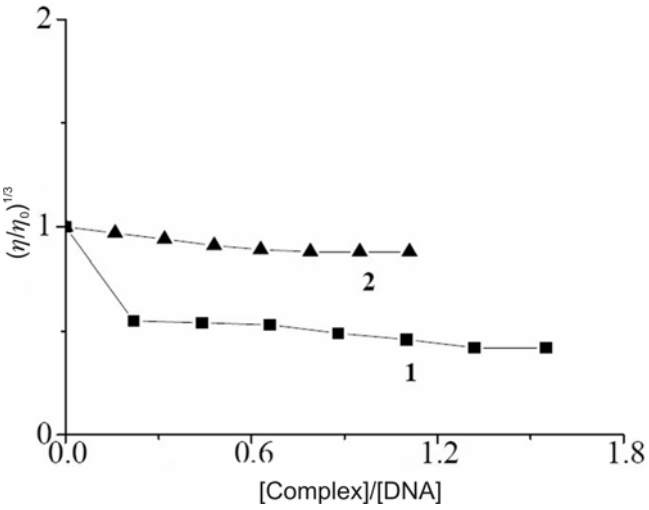

Figure 6. Change in relative specific viscosity of CT–DNA (150 μM) on addition of the complexes **1** (■) and **2** (▲) in 5 mM Tris-HCl buffer medium at 37 ± 0·1°C.

3.3 *Chemical nuclease activity*

The oxidative cleavage of supercoiled (SC) pUC19 DNA (0·2 μg, 30 μM) in 50 mM Tris-HCl/50 mM NaCl buffer (pH, 7·2) by the copper(II) complexes (40 μM) in the presence of a reducing agent, viz. 3-mercaptopropionic acid (MPA, 0·5 mM) has been studied by agarose gel electrophoresis (figure 7). Both the complexes show similar DNA cleavage activity. Control experiments using MPA or the complexes alone do not show any apparent cleavage of SC–DNA. To determine the groove selectivity of the complexes, control experiments have been performed using minor groove binder distamycin and major groove binder methyl green. Addition of distamycin or methyl green does not inhibit the DNA cleavage of the complexes **1** and **2** suggesting their surface binding preference. Control experiments show that the hydroxyl radical scavengers like catalase or DMSO significantly inhibit the DNA cleav-

age activity indicating formation of hydroxyl radical and/or 'copper-oxo' intermediate as the reactive species. SOD addition does not have any apparent effect on the cleavage activity suggesting non-involvement of $O_2^{\bullet-}$ in the cleavage reaction (figure 7). The mechanistic pathway involved in the DNA cleavage reaction could be similar to that proposed by Sigman and coworkers for the 'chemical nuclease' activity of *bis*(phen)copper species.[49,50]

3.4 *DNA and RNA photo-cleavage study*

The photo-induced DNA and RNA cleavage experiments have been carried out in UV-A and red light using the complexes (40 μM for 365 nm and 80 μM for 647·1 nm) and SC pUC19 DNA (0·2 μg, 30 μM) or MG 1655 total tRNA (60 ng per μL) in

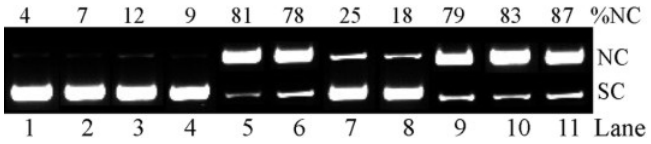

Figure 7. Gel electrophoresis diagram showing the cleavage of SC pUC19 DNA (0·2 μg, 30 μM) by the complexes **1** and **2** (40 μM) in 50 mM Tris-HCl/50 mM NaCl buffer (pH 7·2) in the presence of MPA (0·5 mM): lane 1, DNA control; lane 2, DNA + MPA; lane 3, DNA + **1**; lane 4, DNA + **2**; lane 5, DNA + **1** + MPA; lane 6, DNA + **2** + MPA; lane 7, DNA + catalase (4U) + **1** + MPA; lane 8, DNA + DMSO (4 μL) + **1** + MPA; lane 9, DNA + SOD (4U) + **1** + MPA; lane 10, DNA + distamycin (200 μM) + **1** + MPA; lane 11, DNA + methyl green (200 μM) + **1** + MPA.

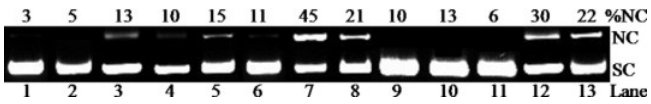

Figure 8. Gel electrophoresis diagram showing the photo-induced oxidative cleavage of SC pUC19 DNA (0·2 μg, 30 μM) and MG 1655 *t*-RNA (60 ng per μL) by **1** and **2** (40 μM for 365 nm and 80 μM for 647·1 nm) and **3** (80 μM for 365 nm) in 50 mM Tris-HCl/NaCl buffer (pH 7·2) on 2 h photo-irradiation with UV-A light of 365 nm and red light of 647·1 nm wavelength: lane 1, DNA control (365 nm); lane 2, DNA + Cu(II) acetate. hydrate (80 μM) (365 nm); lane 3, DNA + H_2RSSR (80 μM) (365 nm); lane 4, DNA + H_2PDS (80 μM) (365 nm); lane 5, DNA + **1** (dark); lane 6, DNA + **2** (dark); lane 7, DNA + **1** (365 nm); lane 8, DNA + **2** (365 nm); lane 9, RNA + **1** (365 nm); lane 10, RNA + **2** (365 nm); lane 11, DNA + **3** (365 nm); lane 12, DNA + **1** (647·1 nm); lane 13, DNA + **2** (647·1 nm).

absence of any external reagent. Complex **1** shows DNA cleavage activity on photo-exposure to both UV-A and red light (figure 8, table 4). Complex **2**, however, exhibits poor photo-induced DNA cleavage activity at 365 nm since it does not have any electronic spectral band near this wavelength. Control experiments using the complexes in dark or the ligands (H_2RSSR and H_2PDS) alone in light do not show any apparent cleavage of the SC DNA at 365 nm. Both the complexes show efficient photo-induced DNA cleavage activity in red light of 647·1 nm. Complex **1** is more active than complex **2** under aerobic reaction conditions. The complexes, however, show similar extent of DNA photo-cleavage activity under argon atmosphere. The cleavage activity in air is found to be higher than that under argon. The observed photoactivity of the complexes could be from photosensitization of the disulphide groups of the ligands in association with the copper(II) centers since the ligands alone are cleavage inactive. The complexes do not show any significant photo-cleavage of RNA. This observation may be attributed to the poor binding propensity of the complexes to RNA. A mixture of DNA and RNA on exposure to UV-A light of 365 nm shows photo-cleavage of only DNA leaving the RNA as intact (figure 9). This observation of selective photo-cleavage of DNA over RNA is significant.

The mechanistic aspects of the DNA cleavage reactions in UV-A and red light have been probed using external additives like sodium azide as singlet oxygen quencher, DMSO and catalase as hydroxyl radical scavengers, and superoxide dismutase (SOD)

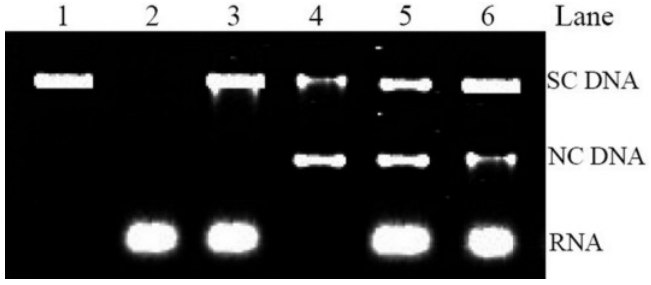

Figure 9. Gel electrophoresis diagram showing the photo-induced cleavage of a mixture of SC pUC19 DNA (0·2 μg, 30 μM) and MG 1655 *t*-RNA (60 ng per μL) (1 : 1 v/v) by **1** and **2** (40 μM) in 50 mM Tris-HCl/NaCl buffer (pH 7·2) on irradiation with UV light of 365 nm wavelength for 2 h: lane 1, DNA control (dark); lane 2, RNA control (dark); lane 3, RNA + DNA + **1** (dark); lane 4, DNA + **1**; lane 5, RNA + DNA + **1**; lane 6, RNA + DNA + **2**.

Table 4. Selected cleavage data of SC pUC19 DNA (0·2 μg, 30 μM NP) and MG1655 *t*-RNA (60 ng per μL) by the complexes **1** and **2**[a].

Sl. No.	Reaction condition	[Complex]/μM	%SC	%NC
Chemical nuclease activity in dark				
1.	DNA + **1**	40	88	12
2.	DNA + **2**	40	91	9
3.	DNA + **1** + MPA	40	19	81
4.	DNA + **2** + MPA	40	22	78
Photo-cleavage of DNA Light source: UV-A light (365 nm, 6 W) in air				
5.	DNA control	–	97	3
6.	DNA + Cu(II) acetate (80 μM)	–	95	5
7.	DNA + H_2RSSR (80 μM)	–	87	13
8.	DNA + H_2PDS (80 μM)	–	90	10
9.	DNA + **1**	40	55	45
10.	DNA + **2**	40	79	21
11.	DNA + **3**	80	94	6
12.	RNA + **1**	40	90	10
Photo-cleavage of DNA light source: red light (647·1 nm CW laser, 100 mW) in air				
13.	DNA control	–	97	3
14.	DNA + **1**	80	70	30
15.	DNA + **2**	80	78	22
Light source: Visible light (647·1 nm CW laser, 100 mW), atmosphere–argon				
16.	DNA control (light)	80	95	5
17.	DNA + **1** (dark)	80	88	12
18.	DNA + **2** (dark)	80	90	10
19.	DNA + **1** (light)	80	74	26
20.	DNA + **2** (light)	80	79	21

[a]SC and NC are supercoiled and nicked circular forms of DNA, respectively. Exposure time was 2 h in UV-A and red light. [MPA] = 0·5 mM

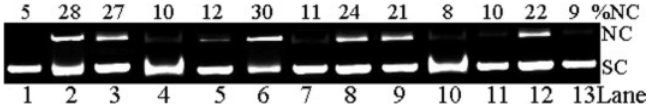

Figure 10. Gel electrophoresis diagram showing the cleavage of SC pUC19 DNA (0·2 μg, 30 μM) by **1** and **2** (80 μM) in the presence of different additives on photo-irradiation at 647·1 nm for 2 h exposure time in 50 mM Tris-Cl/NaCl buffer (pH 7·2): lane 1, DNA control; lane 2, DNA + **1**; lane 3, DNA + NaN_3 (200 μM) + **1**; lane 4, DNA + catalase (4 units) + **1**; lane 5, DNA + DMSO (4 μL) + **1**; lane 6, DNA + D_2O (16 μL) + **1**; lane 7, DNA + SOD (4 units) + **1**; lane 8, DNA + **2**; lane 9, DNA + NaN_3 (200 μM) + **2**; lane 10, DNA + catalase (4 units) + **2**; lane 11, DNA + DMSO (4 μL) + **2**; lane 12, DNA + D_2O (16 μL) + **2**; lane 13, DNA + SOD (4 units) + **2**.

as $O_2^{\bullet-}$ radical scavenger. The reaction has also been carried out in D_2O in which the lifetime of $^1O_2$ is known to be significantly higher than that in water.[51] A significant inhibition of the DNA photo-cleavage has been observed in the presence of catalase, DMSO and SOD suggesting the involvement of hydroxyl and/or superoxide radicals in the DNA photo-cleavage under aerobic conditions (figure 10). No apparent inhibition of DNA photo-cleavage activity is observed in the presence of NaN_3. Addition of D_2O does not have any apparent effect on the cleavage activity. The results exclude the singlet oxygen ($^1O_2$, $^1\Delta_g$) DNA cleavage pathway (type-II process). The DNA cleavage data under aerobic medium suggest the involvement of diffusible $^{\bullet}$OH radicals as the reactive oxygen species (ROS). Under an argon atmosphere, it has been observed that hydroxyl radical scavengers have no apparent effect on the DNA cleavage activity (figure 11, table 4). The DNA photo-cleavage reaction under argon does not involve any ROS. It is likely that formation of a cleavage active species in a type-I pathway involving the disulphide moiety takes place under anaerobic medium. We have probed the effect of solvent on the DNA cleavage activity. It has been

observed that an increase in the concentration of DMF in the DMF-Tris buffer mixture increases the DNA photo-cleavage activity (figure 12). We propose the formation of reactive sulphide anion radical under argon as the active species. It has also been

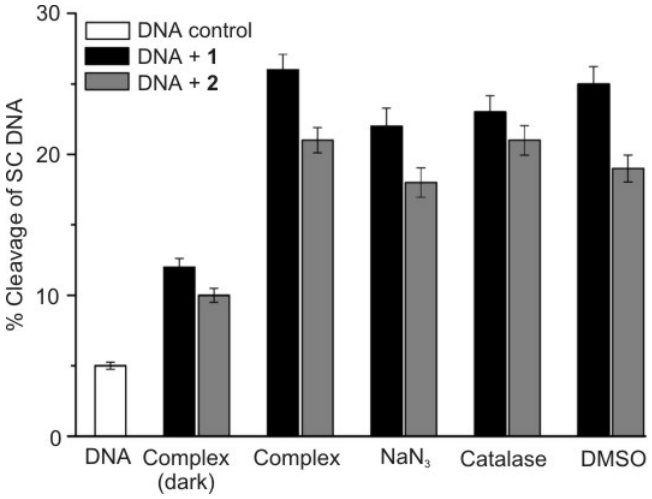

Figure 11. Bar diagram showing the cleavage of SC pUC19 DNA (0·2 μg, 30 μM) by **1** and **2** (40 μM) in the presence of different additives on photo-irradiation at 365 nm for 2 h exposure time in 50 mM Tris-HCl/NaCl buffer (pH 7·2) under argon atmosphere. The additives used are as follows: NaN_3, 200 μM; DMSO, 4 μL; catalase, 4 units.

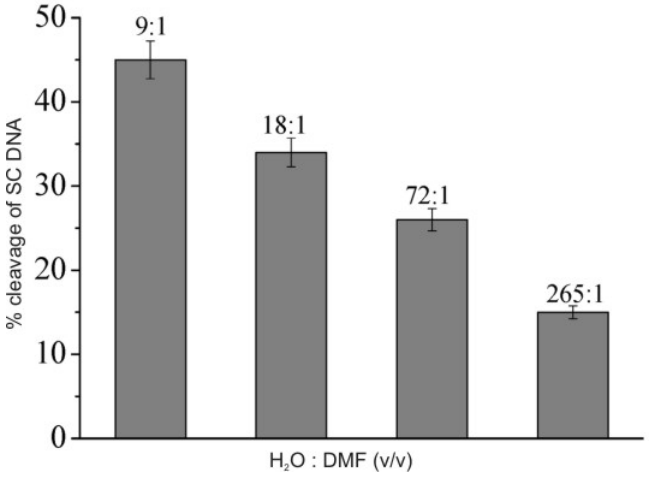

Figure 12. Bar diagram showing cleavage of SC pUC19 DNA (30 μM) by **1** (80 μM, 2 h exposure) under argon on photo-irradiation at 647·1 nm in 50 mM Tris-HCl/NaCl buffer (pH, 7·2) with varying DMF : H_2O (v/v) solvent ratio.

observed that copper(II) complexes having a disulphide moiety show significantly enhanced DNA photo-cleavage activity under anaerobic medium in comparison to the complexes lacking the disulphide bond.[52] In air, it presumably reacts with the dissolved oxygen in the solvent to produce hydroxyl radical.[53] The anaerobic DNA cleavage by sulphide anion radical ($RS^{\bullet-}$) presumably proceeds via formation of nucleobase radical anion ($B^{\bullet-}$) that could activate the sugar moiety by hydrogen abstraction and leading to DNA cleavage.[54,55] The reactions involving the copper(II) complexes seem to be metal-assisted and involve metal-based charge-transfer and ligand field transitions. The observation of less DNA cleavage under anaerobic medium in comparison to that in air could be due to higher diffusion ability of the hydroxyl radicals than the complex bound sulphide anion radicals. The observed difference between the DNA and RNA cleavage could be due to the presence of different sugar moieties and on the ability of $B^{\bullet-}$ in activating the sugar moieties. The diiron(II) complex **3** is found to be inactive in photo-cleaving DNA under similar reaction conditions. The reactions involving the iron(II) complex seem to be energetically unfavourable as we have observed for the photoactive copper(II) and photo-inactive iron(II) complexes of dipyridoquinoxaline.[56]

4. Conclusions

Binuclear copper(II) complexes having ligands with disulphide moiety show anaerobic DNA cleavage activity in red light of 647·1 nm. The disulphide moiety in these copper(II) complexes acts as a photosensitizer effecting light-induced DNA cleavage in air and argon following respective hydroxyl radical and type-I cleavage pathways. The DNA cleavage under argon possibly involves formation of sulphide anion radical species thus making the complexes versatile DNA photo-cleaving agent within the PDT spectral window under both aerobic and hypoxic reaction conditions. The photo-cleavage of DNA by complex **2** is of importance because of the presence of biologically active D-penicillamine moiety in this complex. The conventional PDT agents like Photofrin® require red light, oxygen and a photosensitizer. The cleavage activity of such PDT drugs follows singlet oxygen pathway. Such drugs become inefficient under hypoxic conditions of tumors. The present results showing anaerobic photo-cleavage of DNA in red light are of significance towards designing and developing the chemistry of metal-based PDT agents for cellular applications under hypoxic conditions.

Acknowledgements

We thank the Department of Science and Technology (DST, SR/S5/MBD-02/2007), Government of India, for financial support and the CCD diffractometer facility. We thank Prof. U Varshney, Department of Microbiology and Cell Biology, Indian Institute of Science, Bangalore for MG 1655 total *t*-RNA (isolated from wild type *E. Coli* strain) as a gift. AKP is thankful to Council of Scientific and Industrial Research (CSIR) for a fellowship. We also thank the Alexander von Humboldt Foundation, Germany, for donation of an electroanalytical system. ARC thanks DST for J.C. Bose Fellowship.

References

1. Hara M, Takahashi I, Yoshida M, Asano K, Kawamoto I, Morimoto M and Nakano H 1989 *J. Antibiot.* **42** 333
2. Hara M, Saitoh Y and Nakano H 1990 *Biochemistry* **29** 5676
3. Asai A, Hara M, Kakita S, Kanda Y, Yoshida M, Saito H and Saitoh Y 1996 *J. Am. Chem. Soc.* **118** 6802
4. Chatterjee M, Cramer K D and Townsend C A 1993 *J. Am. Chem. Soc.* **115** 3374
5. Tasaka N T, Matsushita M, Hayashi R, Okonogi K and Itoh K 1993 *Chem. Pharm. Bull.* **41** 1043
6. Kohama Y, Iida K, Semba T, Mimura T, Inada A, Tanaka K and Nakanishi T 1992 *Chem. Pharm. Bull.* **40** 2210
7. Davidson B S, Molinski T F, Barrows L R and Ireland C M 1991 *J. Am. Chem. Soc.* **113** 4709
8. Behroozi S J, Kim W, Dannaldson J and Gates K S 1996 *Biochemistry* **35** 1768
9. Mitra K, Kim W, Daniels J S and Gates K S 1997 *J. Am. Chem. Soc.* **119** 11691
10. Patra A K, Dhar S, Nethaji M and Chakravarty A R 2003 *Chem. Commun.* 1562
11. Dhar S, Senapati D, Das P K, Chattopadhyay P, Nethaji M and Chakravarty A R 2003 *J. Am. Chem. Soc.* **125** 12118
12. Detty M R, Gibson S L and Wagner S J 2004 *J. Med. Chem.* **47** 3897
13. Sessler J L, Hemmi G, Mody T D, Murai T, Burrell A and Young S W 1994 *Acc. Chem. Res.* **27** 43
14. De Rosa M C and Crutchley R J 2002 *Coord. Chem. Rev.* **233–234** 351
15. Bonnett R 2000 *Chemical aspects of photodynamic therapy* (London, UK: Gordon and Breach)
16. Sternberg E D, Dolphin D and Brückner C 1998 *Tetrahedron* **54** 4151
17. Henderson B W, Busch T M, Vaughan L A, Frawley N P, Babich D, Sosa T A, Zollo J D, Dee A S, Cooper M T, Bellnier D A, Greco W R and Oseroff A R 2000 *Cancer Res.* **60** 525
18. Patra A K, Nethaji M and Chakravarty A R 2007 *J. Inorg. Biochem.* **101** 233
19. Dhar S, Nethaji M and Chakravarty A R, 2005 *Inorg. Chem.* **44** 8876
20. Dhar S, Senapati D, Reddy P A N, Das P K and Chakravarty A R 2003 *Chem. Commun.* 2452
21. Roy S, Patra A K, Dhar S and Chakravarty A R 2008 *Inorg. Chem.* **47** 5625
22. Patra A K, Dhar S, Nethaji M and Chakravarty A R 2005 *Dalton Trans.* 896
23. Patra A K, Nethaji M and Chakravarty A R 2005 *Dalton Trans.* 2798
24. Patra A K, Bhowmick T, Ramakumar S and Chakravarty A R 2007 *Inorg. Chem.* **46** 9030
25. Dhar S, Nethaji M and Chakravarty A R 2004 *Dalton Trans.* 4180
26. Dhar S, Nethaji M and Chakravarty A R 2005 *Dalton Trans.* 344
27. Saranak J and Foster K W 2000 *Biochem. Biophys. Res. Commun.* **275** 286
28. Gilbert B C, Silvester S, Walton P H and Whitwood A C 1999 *J. Chem. Soc., Perkin Trans.* **2** 1891
29. Jacob C, Giles G L, Giles N M and Sies H 2003 *Angew. Chem., Int. Ed.* **42** 4742
30. Yasui N and Koide T 2003 *J. Am. Chem. Soc.* **125** 15728
31. Perrin D, Armarego W L F and Perrin D R 1980 *Purification of laboratory chemicals* (Oxford: Pergamon Press)
32. Thich J A, Mastropaolo D, Potenza J and Schugar H J 1974 *J. Am. Chem. Soc.* **96** 726
33. Kahn O 1993 *Molecular magnetism* (Weinheim, Germany: VCH)
34. Bleaney B and Bowers K D 1952 *Proc. R. Soc. London, Ser.* **A214** 451
35. Walker N and Stuart D 1983 *Acta Crystallogr.* **A39** 158
36. Sheldrick G M, 1997 *SHELX-97, Programs for crystal structure solution and refinement* (Göttingen, Germany: University of Göttingen)
37. Burnett M N and Johnson C K 1996 *ORTEP-III, Report ORNL-6895* (Oak Ridge, TN: Oak Ridge National Laboratory)
38. Reichman M E, Rice S A, Thomas C A and Doty P 1954 *J. Am. Chem. Soc.* **76** 3047
39. McGhee J D and von Hippel P H 1974 *J. Mol. Biol.* **86** 469
40. Carter M T, Rodriguez M and Bard A J 1989 *J. Am. Chem. Soc.* **111** 8901
41. Cohen G and Eisenberg H 1969 *Biopolymers* **8** 45
42. Bernadou J, Pratviel G, Bennis F, Girardet M and Meunier B 1989 *Biochemistry* **28** 7268
43. Barton J K, Danishefsky A T and Goldberg J M 1984 *J. Am. Chem. Soc.* **106** 2172
44. Gunther L E and Yong A S 1968 *J. Am. Chem. Soc.* **90** 7323
45. An Y, Liu S-D, Deng S-Y, Ji L-N and Mao Z-W 2006 *J. Inorg. Biochem.* **100** 1586
46. Veal J M and Rill R L 1991 *Biochemistry* **30** 1132
47. Satyanarayana S, Dabrowiak J C and Chaires J B 1993 *Biochemistry* **32** 2573

48. Wittung P, Nielsen P and Norden B 1996 *J. Am. Chem. Soc.* **118** 7049
49. Zelenko O, Gallagher J and Sigman D S 1997 *Angew. Chem. Int. Ed. Engl.* **36** 2776
50. Thederahn T B, Kuwabara M D, Larsen T A and Sigman D S 1989 *J. Am. Chem. Soc.* **111** 4941
51. Khan A U 1976 *J. Phys. Chem.* **80** 2219
52. Lahiri D, Bhowmick T, Pathak B, Shameema O, Patra A K, Ramakumar S and Chakravarty A R 2009 *Inorg. Chem.* **48** 339
53. Tanaka M, Ohkubo K and Fukuzumi S 2006 *J. Am. Chem. Soc.* **128** 12372
54. Burrows C J and Muller J G 1998 *Chem. Rev.* **98** 1109
55. Szacilowski K, Macyk W, Drzewiecka-Matusek A, Brindell M and Stochel G 2005 *Chem. Rev.* **105** 2647
56. Roy M, Pathak B, Patra A K, Jemmis E D, Nethaji M and Chakravarty A R 2007 *Inorg. Chem.* **46** 11122